

Sequential and cotunneling behavior in the temperature-dependent thermopower of few-electron quantum dots

R. Scheibner,¹ E. G. Novik,¹ T. Borzenko,¹ M. König,¹ D. Reuter,² A. D. Wieck,² H. Buhmann,¹ and L. W. Molenkamp¹

¹Physikalisches Institut (EP3), Universität Würzburg, Am Hubland, 97074 Würzburg, Germany

²Lehrstuhl für Angewandte Festkörperphysik, Ruhr-Universität Bochum, Universitätsstraße 150, 44780 Bochum, Germany

(Received 8 August 2006; revised manuscript received 11 October 2006; published 2 January 2007)

We have studied the temperature-dependent thermopower of gate-defined, lateral quantum dots in the Coulomb blockade regime using an electron heating technique. The line shape of the thermopower oscillations depends strongly on the contributing tunneling processes. Between 1.5 K and 40 mK a crossover from a pure sawtooth to an intermittent sawtoothlike line shape is observed. The latter is attributed to the increasing dominance of cotunneling processes in the Coulomb blockade regime at low temperatures.

DOI: [10.1103/PhysRevB.75.041301](https://doi.org/10.1103/PhysRevB.75.041301)

PACS number(s): 73.50.Lw, 73.23.Hk, 73.63.Kv

The perspective of scalable semiconductor quantum processing devices feeds an intense interest in quantum dot (QD) structures that contain only a few electrons.¹ For the development of these devices, a detailed knowledge of the underlying electron transport processes is of crucial importance. So far, most of the transport experiments have focused on the electrical conductance.² Although thermoelectrical transport measurements are known to be more sensitive to the details of the electronic structure than conventional transport measurements,³ little experimental attention has been paid to this kind of measurement on QDs. Within the scope of the Onsager relations, the thermopower S , which is given by

$$S \equiv - \lim_{\Delta T \rightarrow 0} \frac{V_T}{\Delta T} \Big|_{I=0} = - \frac{\langle E \rangle}{eT}, \quad (1)$$

relates the average energy $\langle E \rangle$ transfer at a temperature T to the thermovoltage V_T for a given temperature difference ΔT across the device at zero net current. This additional information about the carrier kinetics is not provided by conventional transport measurements and helps to distinguish between different possible transport regimes.⁴

In the past, thermopower measurements on QDs in the Coulomb blockade (CB) regime have yielded qualitatively different results: either a sawtoothlike line shape, or a line shape similar to the derivative of a single-electron-tunneling (SET) conductance peak is observed when the electrochemical potential is varied in order to change the number of electrons occupying the QD. So far, a sawtoothlike behavior has been observed mainly for many-electron QDs, while derivativelike line shapes are predominantly reported for smaller QDs at low (millikelvin) temperatures.⁵⁻⁷

Here, we present thermovoltage measurements on gate-defined, lateral QDs, containing a few tens of electrons, which allow us to analyze the low-temperature line shape profile in detail. For a series of SET conductance peaks, the transition is observed from a full sawtooth line shape to a sawtooth with an intermittent periodic zero thermovoltage signal while the temperature is lowered from $T=1.5$ K to $T < 100$ mK. This behavior is in qualitative agreement with recent theoretical considerations of Turek and Matveev⁸ for many-electron QDs. The transition is associated with an in-

creasing dominance of cotunneling processes for decreasing temperatures. In our measurements we find that the regime of sequential tunneling, which dominates the transport in the vicinity of the SET conductance peaks, extends much further than anticipated for many-electron dots. This leads to an enhanced absolute thermopower for few-electron devices.

The measurements are carried out in a top-loading dilution refrigerator at lattice temperatures between 40 mK and 1.5 K. The GaAs/(Al,Ga)As QDs are fabricated by split-gate technology using optical and electron-beam lithography. The two-dimensional electron gas is located 70 nm below the surface, and has a carrier density $n_e=2.3 \times 10^{15} \text{ m}^{-2}$ and a mobility $\mu=100 \text{ m}^2/(\text{Vs})$. The gate structure of the samples is shown in Fig. 1.⁹ Gates A, D, E, and F form the QD with a nominal diameter of approximately 250 nm. The voltage applied to the plunger gate E, V_E , is used to control the number of electrons on the QD. Low-frequency lock-in techniques are used for the transport experiments. The effective charging energy E_C^* is determined from finite-bias conductance measurements. In the regime where CB oscillations are observable, E_C^* decreases from 3.0 to 0.8 meV when the coupling to the reservoirs is increased.

Gates B and C define, together with gates A and D, the electron heating channel, and, at the same time, the reference quantum point contact (QPC_{ref}) in the thermopower experiments.^{10,11} Using the electron heating technique, only the diffusion (electronic) contribution to the thermopower is probed. By adjusting the conductance of QPC_{ref} to the center of a quantized plateau, its thermopower is approximately zero, $S_{\text{QPC}_{\text{ref}}} \approx 0$. The transverse voltage $V_T \equiv V_1 - V_2$ (cf. Fig. 1) is then directly proportional to the thermopower of the QD. A constant temperature difference across the dot is

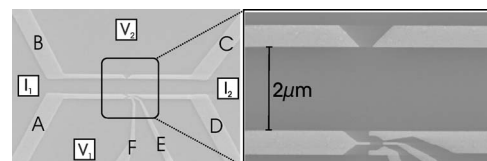


FIG. 1. Scanning electron microscope image of the sample structure. Schottky gates are labeled A, B, ..., F. Sample areas that serve as current and voltage contacts are labeled I_1 , I_2 and V_1 , V_2 , respectively.

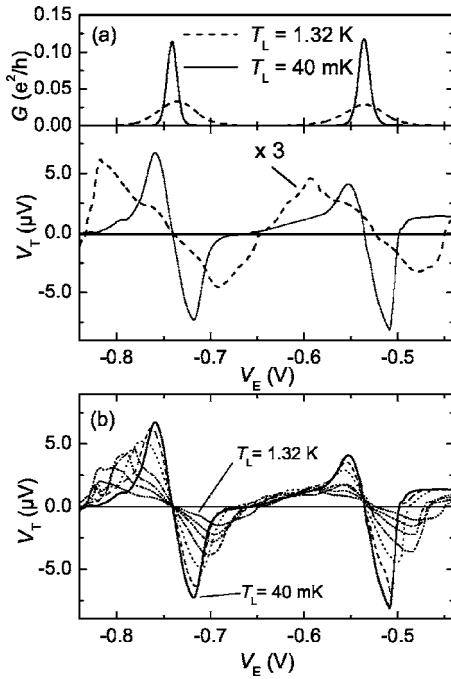


FIG. 2. (a) Conductance G (upper panel) and the corresponding thermovoltage V_T (lower panel) of QD1 as a function of the plunger-gate voltage V_E . (b) Thermovoltage at seven different temperatures [from low temperatures (large signal amplitude) to high temperatures (small signal amplitude)]: $T_L = 40$ mK (solid), 66 mK (dash), 158 mK (dot), 257 mK (dash-dot), 425 mK (dash-dot-dot), 1.04 K (short dash), and 1.5 K (short dot).

maintained by passing an ac current of $\nu = 13$ Hz through the heating channel. V_T is detected at twice the excitation frequency (26 Hz). Here, we discuss two QD samples (QD1 and QD2) that have the same gate structure design but adjusted to have a different number of electrons; QD1 (QD2) contains between 15 (30) and 20 (40) electrons. A constant ac current of $I_H = 9.7$ nA (4.2 nA) increases the electron temperature in the heating channel by $\Delta T = 9$ mK (3 mK) for QD1 (QD2) in the whole temperature range.

Figure 2(a) shows the conductance G and the corresponding thermovoltage V_T of QD1 for an electrostatic charging energy $E_C = 1.43$ meV at lattice temperatures $T_L = 40$ mK (black lines) and 1.32 K (gray lines). At 1.32 K, thermal broadening determines the shape of the SET conductance peaks. The corresponding thermovoltage signal shows a sawtoothlike line shape with a maximum in the vicinity of the center of the CB. Additional fine structure on the sawtooth line shape which is even visible at elevated temperatures is due to the finite level spacings in the QD. At $T_L = 40$ mK, the SET conductance peaks have an increased height and a reduced width, and are well separated by regimes of (approximately) zero conductance. The line shape of the corresponding thermovoltage now resembles more the negative derivative of the conductance G . The values of the thermovoltage extrema have increased by a factor of 3 and their positions are shifted toward the SET conductance peaks.

A small asymmetry between the thermovoltage values of positive and negative amplitude is observed for all measurements. This asymmetry is reduced for more negative plunger

gate voltages V_E (cf. Figs. 2 and 4). The asymmetry in the thermovoltage is intrinsic and is attributed to the energy-dependent transmission probability of the tunnel barriers and possible multichannel tunneling processes.¹² Similarly, the observation of additional long shoulders in the thermovoltage for the SET conductance peak at $V_E = -0.54$ V can be attributed to an imbalance of tunnel processes from above and below the Fermi energy. We have reported similar features previously in the spin-correlated transport regime.⁴

Figure 2(b) shows V_T for seven different temperatures in the range from $T_L = 1.32$ K down to 40 mK. It is evident that the change in line shape occurs continuously. In the vicinity of the SET conductance peaks the thermovoltage varies linearly with V_E , its slope increases with decreasing T while in between the SET conductance peaks, a region where $V_T \approx 0$ develops. The observation of two different line shapes indicates that at different temperatures different transport mechanisms dominate the electronic transport properties.

Near the SET conductance peaks, the charge transport is dominated by sequential tunneling (ST) processes and is explained within the so-called orthodox model,¹³ where only first-order tunneling processes are considered. Between the SET conductance peaks, the transport can also be due to ST processes, but only at relatively high temperatures (~ 1 K). In ST transport, the average electron energy is proportional to an effective energy gap E_g which is defined as the difference between the Fermi energy of the leads and the energy of the closest QD state. E_g varies linearly between $-E_C^*/2$ and $+E_C^*/2$ with increasing electrochemical potential of the QD, Φ_{QD} , and subsequently jumps back to $-E_C^*/2$ at the center of the CB. According to Eq. (1), the thermovoltage follows this sawtoothlike behavior. Thermal smearing at higher temperatures leads to a more sinusoidal variation of E_g and thus the maxima of the thermovoltage oscillations are located slightly away from the center of the CB. The ST mechanism thus explains the line shape at temperatures around 1 K.

We attribute the low (millikelvin) temperature line shape to the occurrence of (inelastic) cotunneling (CT) transport in between the SET conductance peaks.⁸ At low temperatures, these higher-order processes dominate the transport away from the SET conductance peaks, because the ST processes are thermally activated and thus exponentially suppressed on lowering the temperature, while CT processes scale only according to a power law.¹⁴ Due to energy conservation, the average energy transferred by cotunneling processes is proportional to the temperature ($\langle E_{Co} \rangle \propto T$). Therefore, the expected thermoelectric signal of CT processes is vanishingly small.⁸ Decreasing the sample temperature implies a transition from ST- to CT-dominated transport in the CB regime away from the SET conductance peaks and thus a suppression of the thermovoltage signal in the corresponding gate voltage ranges. The sawtooth line shape becomes interrupted by regions of (nearly) zero signal amplitude, as observed in Fig. 2. However, if contributions of cotunneling processes from above and below the Fermi energy are not symmetric a finite nonzero thermovoltage will be observable in the experiments (see Fig. 2).

In order to discuss this transition more quantitatively we compare the thermovoltage oscillation at $V_E = -0.73$ V with the behavior of the orthodox (pure ST) model,¹³ and a model

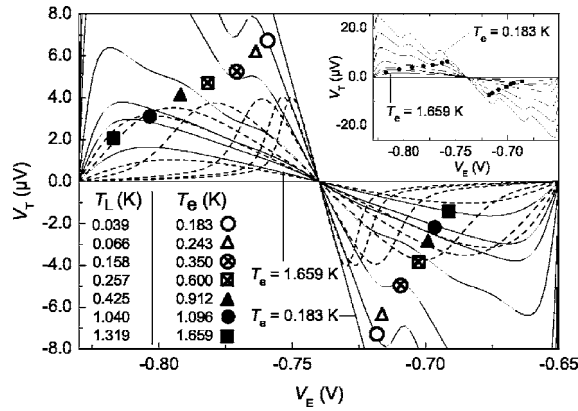


FIG. 3. Calculated thermovoltage as a function of V_E for the orthodox (solid lines) and CT-included model (dashed lines). The symbols indicate the maxima of the measured thermovoltage signal for the corresponding temperatures, which are listed in the figure. The inset shows the orthodox model at full scale (solid lines) together with the maxima of the measured thermovoltage signal (marked as dots).

that also includes CT effects.⁸ At $T_L=1.32$ K both models exhibit nearly the same thermovoltage amplitude and approximately the same line shape (see Fig. 3). For this temperature, our QD satisfies the condition $\hbar\Gamma \ll k_B T \ll E_C$, which allows us to extract the relevant model parameters. We obtain $E_C^* = 1.712$ meV, $\alpha = \Phi_{QD}/(-eV_E) = 0.0095$, and $G_{l,r} = 0.072e^2/h$, where $G_{l,r}$ ($\propto \hbar\Gamma$) describes the tunnel conductance to the left and right reservoirs, respectively. Considering these parameters as temperature independent we calculate the temperature-dependent thermovoltage (Fig. 3). Since the charging energy of the QD determines the slope of the thermovoltage signal in the close vicinity of the SET conductance peaks, the direct comparison with the experiment allows us to extract the effective electron temperature T_E under our experimental conditions. The deduced values for T_E are shown in Fig. 3 and have been confirmed independently by fitting the conductance peaks.^{15,16} For clarity, only the maxima of the measured thermovoltage are indicated in the figure, together with the results of the model calculations.

In the orthodox model, a sawtooth line shape is predicted for all temperatures (Fig. 3). The wiggles on the declining slope of the sawtooth originate from excited states and have the periodicity of the level spacing. At the same time, the CT-included model does indeed reproduce a transition from a sawtooth to a periodically suppressed sawtooth line shape. However, while the CT-included model predicts an approximately constant peak amplitude, the experiments show a strong increase in peak amplitude with decreasing temperature. In addition, the model does not predict the gate-voltage position of the maxima correctly. A comparison of Figs. 2 and 3 reveals that in the experiment the linear increase of the thermovoltage around the SET conductance peaks extends much further than anticipated by the CT-included model, and rather follows the behavior of the orthodox model, i.e., the voltage range where ST dominates the transport is larger than given by the CT-included model. In other words, the present CT-included model does not describe quantitatively the influence of CT processes for our few-electron QD. The reason

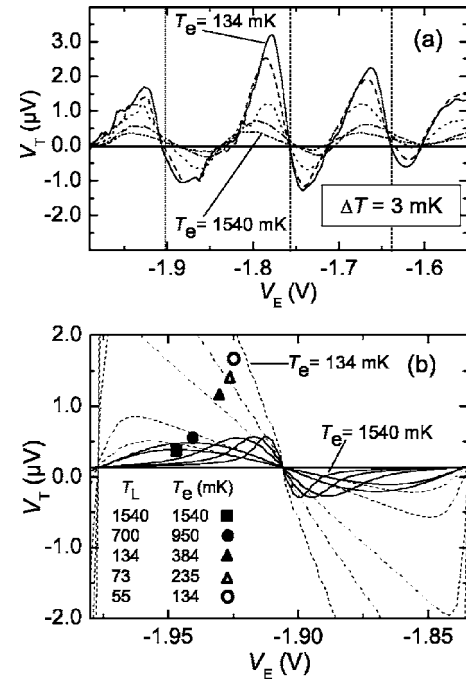


FIG. 4. (a) Thermovoltage of QD2 as a function of the plunger-gate voltage V_E for a series of SET conductance peaks. The positions of the SET conductance peaks are indicated by vertical dashed lines. From low temperatures (large signal amplitude) to high temperatures (small signal amplitude): $T_{e(L)} = 134$ (55) mK (solid), 235 (73) mK (dash), 384 (134) mK (dot), 950 (700) mK (dash-dot), and 1540 (1540) mK (dash-dot-dot). (b) Calculated thermovoltage as a function of V_E for the orthodox (dashed lines) and CT-included model (solid lines). Symbols indicate the maxima of the measured thermovoltage signal near the SET conductance peaks at $V_E = -1.9$ V for the corresponding temperatures (listed in the figure).

is that the CT-included model assumes a negligible energy spacing of the QD states ($\delta E_{QD} \ll k_B T$), as applicable for metallic dots. For the present few-electron QD δE_{QD} clearly is not negligible; the energy gap between the ground and the first excited state is of the order of 250 μ eV. Even at temperatures around 1 K, only a few excited states are available for transport, which reduces the probability for cotunnel events.

Additionally, we measured a second QD sample, which has the same layout as QD1 (see Fig. 1). QD2 exhibits a similar charging energy ($E_C^* \approx 1.5$ meV) but smaller level spacing ($\delta E \sim 50$ μ eV) presumably due to variations in the individual potential landscape in the 2DEG.¹⁷ This sample is further into the many electron limit and exhibits a very strong coupling of the QD states to the leads. Thus one would expect stronger cotunneling contributions to the thermopower. However, a similar behavior as for QD1 is observed. Figure 4(a) shows the change of the thermovoltage line shape for a series of SET conductance peaks. A change in line shape with temperature is present. It can be identified by the shift of the thermovoltage extremal values toward the positions of the SET conductance peaks and by the appearance of a plateaulike structure at $V_E = -1.85$ V for low temperatures. The change in line shape becomes less pronounced for more positive gate voltages, where the coupling of the

QD states to the leads increases considerably. Since the used theoretical models are not really applicable for the strong coupling limit ($V_E > -1.85$ V), the line shape close to the SET conductance peak at $V_E = -1.9$ V has been used to evaluate the model calculations similar to QD1. Figure 4(b) shows that again the regime of sequential tunneling is extended with respect to the expected curves using the CT-included model.

In summary, the thermopower of few-electron QDs reveals a transition of the line shape as a function of the QD potential from a full sawtooth to an intermittent sawtooth behavior. This transition is directly related to a change in the dominant transport processes. While close to the SET conductance peaks, sequential tunneling processes dominate, the

full CB regime is dominated by inelastic cotunneling processes. Compared with many-electron (metallic) QDs, the regime of sequential tunneling is extended to a wider gate-voltage range for few-electron QDs, which results in an increasing thermopower peak amplitude with decreasing temperature even in the presence of cotunneling processes. It will be interesting to look for these effects in QDs in the very-few-electron limit.⁹

We wish to thank C. Gould and J. Weis for valuable discussions. We gratefully acknowledge the financial support of the DFG (Grant No. Mo771/5-2) and the Office of Naval Research (Grant No. 04PR03936-00).

-
- ¹D. Loss and D. P. DiVincenzo, *Phys. Rev. A* **57**, 120 (1998).
²L. P. Kouwenhoven, C. M. Marcus, P. L. McEuen, S. Tarucha, R. M. Westervelt, and N. S. Wingreen, *Mesoscopic Electron Transport* (Kluwer Academic, Dordrecht, 1997), pp. 105–214.
³J. M. Ziman, *Electrons and Phonons* (Oxford University Press, Oxford, U.K., 1960).
⁴R. Scheibner, H. Buhmann, D. Reuter, M. N. Kiselev, and L. W. Molenkamp, *Phys. Rev. Lett.* **95**, 176602 (2005).
⁵A. A. M. Staring, L. W. Molenkamp, B. W. Alphenaar, H. van Houten, O. J. A. Buyk, M. A. A. Mabesoone, C. W. J. Beenakker, and C. T. Foxon, *Europhys. Lett.* **22**, 57 (1993).
⁶S. Möller, H. Buhmann, S. F. Godijn, and L. W. Molenkamp, *Phys. Rev. Lett.* **81**, 5197 (1998); S. F. Godijn, S. Möller, H. Buhmann, L. W. Molenkamp, and S. A. vanLangen, *ibid.* **82**, 2927 (1999).
⁷A. S. Dzurak, C. G. Smith, C. H. W. Barnes, M. Pepper, L. Martin-Moreno, C. T. Liang, D. A. Ritchie, and G. A. C. Jones, *Phys. Rev. B* **55**, R10197 (1997).
⁸M. Turek and K. A. Matveev, *Phys. Rev. B* **65**, 115332 (2002).
⁹M. Ciorga, A. S. Sachrajda, P. Hawrylak, C. Gould, P. Zawadzki, S. Jullian, Y. Feng, and Z. Wasilewski, *Phys. Rev. B* **61**, R16315 (2000).
¹⁰B. L. Gallagher, T. Galloway, P. Beton, J. P. Oxley, S. P. Beaumont, S. Thoms, and C. D. W. Wilkinson, *Phys. Rev. Lett.* **64**, 2058 (1990); L. W. Molenkamp, Th. Gravier, H. van Houten, O. J. A. Buijk, M. A. A. Mabesoone, and C. T. Foxon, *ibid.* **68**, 3765 (1992).
¹¹H. van Houten, L. W. Molenkamp, C. W. J. Beenakker, and C. T. Foxon, *Semicond. Sci. Technol.* **7**, B215 (1992); P. Streda, *J. Phys.: Condens. Matter* **1**, 1025 (1989); L. W. Molenkamp, H. van Houten, C. W. J. Beenakker, R. Eppenga, and C. T. Foxon, *Phys. Rev. Lett.* **65**, 1052 (1990).
¹²S.-J. Xiong and Y. Yin, *Phys. Rev. B* **66**, 153315 (2002); S.-J. Xiong and Y. Xiong, *Phys. Rev. Lett.* **83**, 1407 (1999).
¹³C. W. J. Beenakker and A. A. M. Staring, *Phys. Rev. B* **46**, 9667 (1992).
¹⁴D. V. Averin and Yu. V. Nazarov, *Phys. Rev. Lett.* **65**, 2446 (1990).
¹⁵C. W. J. Beenakker, *Phys. Rev. B* **44**, 1646 (1991).
¹⁶S. Vorotjsov, *Int. J. Mod. Phys. B* **18**, 3915 (2004).
¹⁷J. J. Koonen, H. Buhmann, and L. W. Molenkamp, *Phys. Rev. Lett.* **84**, 2473 (2000).